Anaglyph Image Generation by Matching Color Appearance Attributes

Songnan Li, Lin Ma, and King Ngi Ngan, Fellow, IEEE

Department of Electronic Engineering, The Chinese University of Hong Kong

Abstract

Anaglyph is an inexpensive three-dimensional (3D) displaying technique. It has deficiencies like color distortions, retinal rivalry, ghosting effect, etc. In this paper, a new method is proposed for anaglyph image generation. In contrast to most existing studies which focus on solving part of the problems, the proposed method tries to minimize the color distortions, retinal rivalry, and ghosting effect simultaneously. It works in the CIELAB color space which is perceptually uniform. Rather than matching the L*a*b* values of the stereo image pair and the perceived anaglyph image as in an existing method [1], the proposed algorithm is aimed at matching perceptual color appearance attributes which can accurately define the color perception of the human visual system (HVS). Rather than evaluating the performance based on typically 3 to 5 images as in most prior studies, subjective tests have been conducted, involving 25 stereo image pairs and 20 subjects, to compare four anaglyph generation methods. The proposed method demonstrates a very good performance for most of the images in the subjective test.

Keywords: Anaglyph, CIELAB color space, color appearance attributes, subjective test

1. Introduction

Among many three-dimensional (3D) displaying techniques, e.g., glasses dependent or auto-stereoscopic [2], anaglyph is the least expensive way to make the 3D visual experience achievable on ordinary monitors or even prints [3], with no special hardware but only cheap colored glasses. Despite of its many inherent deficiencies, its resurgence has been seen recently thanks to

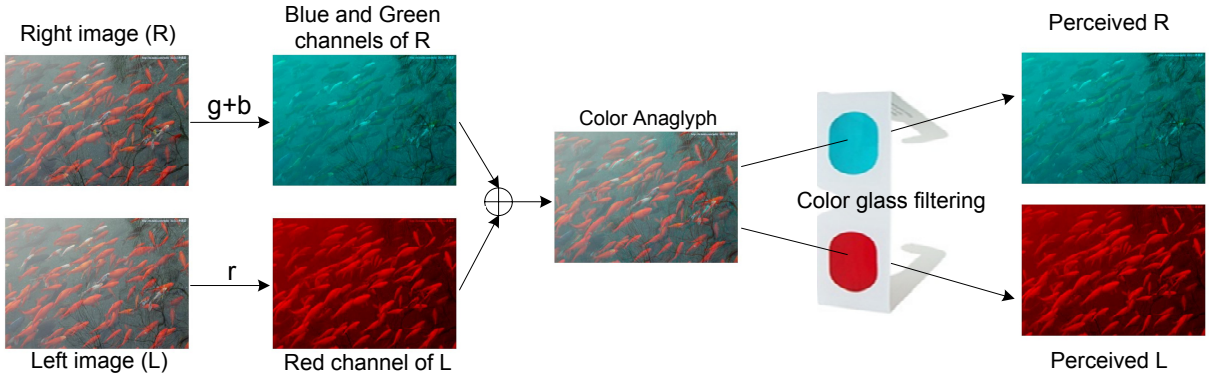

Figure 1: An illustration of anaglyph 3D displaying using Color anaglyph.

the abundance of 3D content which is more easily accessible nowadays than ever.

Like other 3D displaying techniques, anaglyph can provide a slightly different view to each of two eyes. From the disparity between the two views and other visual cues [4], the human visual system can generate the stereoscopic representation of spatial relationships in the scene. An anaglyph image is formed by superimposing two views (i.e., left and right images of a stereo image pair) in different colors. When perceived through colored glasses, the two images will be separated from the composite one to feed each eye. The separation is based on color filtering as has been elaborated in the literature [5, 6]. Figure 1 illustrates how anaglyph works using the most popular and simplest anaglyph method, i.e., Color anaglyph. As shown in Figure 1, a red-cyan Color anaglyph image is generated by combining the red channel $\{R_l^{'}\}$[1] of the left image and the blue & green channels $\{G_r^{'}, B_r^{'}\}$ of the right image together, i.e., $\{R_l^{'}, G_r^{'}, B_r^{'}\}$. Wearing red-cyan colored glasses, the left eye perceives $\{R_l^{'}\}$ since the red lens blocks most of the green and blue colors. And the right eye perceives $\{G_r^{'}, B_r^{'}\}$ due to the opposite color filtering property of the cyan lens.

Anaglyph images mainly suffer from three deficiencies, i.e., color distortions, retinal rivalry, and ghosting effect. Color distortions cause the colors perceived through the glasses to be quite different from those of the original scene. This can be observed from Figure 1 by comparing the original

[1]The 'prime' symbol denotes gamma-corrected signals.

stereo pair with the simulated perception of the two eyes. Retinal rivalry occurs when the same object appears to have different colors in the two eyes. This phenomenon can be observed from Figure 1 by comparing the simulated perception of the two eyes. Retinal rivalry is distracting, and causes visual fatigue and other side effects [1]. As the color gamuts of our eyes behind the colored glasses do not overlap [1], retinal rivalry is inevitable. However, by manipulating the lightness, retinal rivalry can be significantly reduced. Shown as an example above, Color anaglyph does not attempt to control the retinal rivalry effect in its formation. It is evident from Figure 1 that fishes perceived by the left eye are much brighter than those of the right eye. Under this circumstance the retinal rivalry will be extremely severe. Ghosting is a common problem for most 3D displaying techniques [7, 8]. In anaglyph, ghosting is caused by the imperfect filtering of the light wavelengths, so that the unwanted image leaks through the colored glasses mixing with the intended one. It is often more obvious in regions where there is a striking contrast and a large binocular disparity.

In this paper, a new algorithm is proposed for anaglyph image generation, with explicit considerations for lessening color distortions, retinal rivalry, and ghosting effect. The study is based on liquid crystal displays (LCDs) and red-cyan colored glasses. But the principle can also be applied to other types of displays, e.g., cathode ray tube (CRTs), plasma display panels (PDPs), digital light processors (DLPs) etc., and other colored glasses, e.g., green-magenta (Trioscopic 3D) [9], yellow-blue (ColorCode 3D) [10] etc. The main reason for investigating red-cyan anaglyph is that (1) the technique is patent free, and (2) the performance can be compared with existing work in the literature most of which also studied red-cyan anaglyph. Recently, alternatives to typical anaglyph colors have been proposed. For example, in magenta-cyan anaglyph [11] two primary colors are used to present each view. According to [11], in comparison to red-cyan anaglyph the additional blue color for the left view can help to reduce the retinal rivalry effect and preserve the color accuracy. White-white anaglyph (Infitec Dualcolor3D) [12] was developed using narrow-band interference filters. The new technique can deliver full colors to each eye similar to polarization or shutter glasses based methods. But it cannot be applied to standard display monitors. These alternative methods are beyond the scope of our study.

This paper is structured as follows. In Section 2, brief reviews are given on existing studies of anaglyph generation algorithms. The motivation and novelty of the proposed method is also explained. Section 3 introduces

a detailed implementation of the proposed method. Section 4 shows our experimental results. Finally, conclusion is given in Section 5.

2. Related Work

2.1. Simple anaglyphs

In this paper, simple anaglyphs refer to those methods which disregard properties of display and colored glasses. Representatives include Color anaglyph, Half Color anaglyph, Optimized anaglyph, etc., as formulated in [13]. According to the performance comparison in [13] based on five images of natural scenes, Color anaglyph seems to demonstrate the least color distortions, but on the other hand produces severe retinal rivalry, similar to our observation in Figure 1. Half Color anaglyph and Optimized anaglyph address the retinal rivalry problem at the expense of color reproduction. For example, it has been claimed in [13] that Optimized anaglyph is almost free of luminance retinal rivalry, whereas produces no red shades. Simple anaglyphs are easy to implement and may perform well in many cases. However, they are empirical methods, leaving us with no means to fine-tune their behaviors in accordance with properties of the display and colored glasses to achieve the superior performance.

2.2. XYZ and LAB anaglyphs

Dubois [5] proposed an anaglyph generation method, named as XYZ anaglyph in this paper, which takes into account spectral distributions of display primaries and transmission functions of the colored glasses. In general, the principle of XYZ anaglyph is to minimize the color distortions, i.e., differences between the perception of the original stereo pair and that of the anaglyph image through the colored glasses, in the CIE 1931 XYZ color space. It can be formulated as:

$$min_{_{V_A}} ||C \times V - C_A \times V_A|| \tag{1}$$

where $\times$ denotes matrix multiplication. In (1), $V = [R_l, G_l, B_l, R_r, G_r, B_r]^T$ represents a pixel of the stereo pair[2], $V_A = [R_A, G_A, B_A]^T$ is the corresponding pixel in the anaglyph image, C is a 6×6 matrix converting V from the

[2]The RGB values have gone through the display gamma, and have been normalized to 1.

device RGB color space into the CIE XYZ color space, and C_A is a 6×3 matrix whose multiplication with V_A serves two purposes, i.e., simulating the filtering of the colored glasses and converting the passing lights into the CIE XYZ color space. Element values of matrices C and C_A are determined by spectral distributions of display primaries, and additionally C_A is also dependent on transmission functions of the glasses. Since the color space conversion from RGB to CIE XYZ is linear and the distance between two XYZ colors is measured by the l_2 norm (Euclidean distance), Eq. (1) has a closed form solution, i.e., $V_A = (C_A^T \times C_A)^{-1} \times C_A^T \times V$, which means that XYZ anaglyph actually is as efficient as the simple anaglyphs introduced above, if disregarding the display gamma transfer. It should be noted that V_A calculated in this way will fall out of the gamut of the device RGB color space. Hence, a scaling of V_A is required, followed by a clipping to ensure that the final results lie inside the unit RGB cube. A similar approach was proposed in [14], which still calculates the color distortions in the CIE XYZ space but replaces the l_2 norm in Eq. (1) with l_∞ norm (Chebychev distance). The resultant method requires solving a linear program for each pixel of the anaglyph image, thus is quite time-consuming. The authors exploited color coherence and parallel processing to accelerate the execution.

Recently, McAllister et al. [1] proposed an anaglyph method, namely LAB anaglyph, minimizing the color distortions in the CIELAB color space. Compared to CIE XYZ, the CIELAB color space exhibits several major advantages: (a) it is regarded as a uniform color space, i.e., the Euclidean distance in the CIELAB color space correlates well with the perceptual color distance; (b) it incorporates chromatic adaptation transform and non-linear response compression [15] to more accurately simulate the perception of the human visual system (HVS); (c) it provides means for transforming tri-stimulus values to several color appearance attributes, i.e., lightness, saturation, hue, etc. In the LAB anaglyph [1], V and V_A in (1) are converted into the CIELAB color space. This color space conversion is non-linear, hence as in [14] the resultant formula needs to be optimized iteratively.

2.3. Ghosting reduction methods

Woods et al. [6] discussed in detail the source of the anaglyph ghosting. In [16], three methods were proposed to reduce ghosting, i.e., stereo pair registration, color component blurring, and depth manipulation. In [17], the authors proposed to inhibit ghosting by controlling the amount of saturation.

In [18], ghosting reduction was implemented in a sequential process, i.e., analyzing differences between the left and right images, detecting the ghosting area, and eventually adjusting the intensities of the ghosting area. Tran [19] proposed ghosting reduction methods which relied on explicit knowledge of properties of the display device and the colored glasses. They can serve as post-processing components for existing anaglyph algorithms. Recently, Sanftmann et al. [20] defined a model to quantify the perceived luminance through the colored glasses. Five parameters of the model can be captured by simple subjective tests. Illustration was given on how to use the model together with several simple anaglyph methods to reduce the ghosting artifacts.

2.4. Motivation and novelty

The proposed method is mainly inspired by XYZ and LAB anaglyph methods. As aforementioned, XYZ and LAB anaglyph methods try to minimize the Euclidian distance between original and perceived colors in the CIE XYZ and CIELAB color spaces, respectively. Similarly, the proposed method also aims at minimizing the perceptual differences between the original and perceived colors. But instead of using the XYZ or L*a*b* values, our method is based on matching the semantically meaningful color appearance attributes, i.e., lightness, saturation, and hue. According to [15], color appearance attributes are deemed to be the color representations in the late stage of HVS. They can be used to accurately define the HVS color perception. Therefore, anaglyph methods based on color appearance attributes have the potential to lead to superior performance.

As the LAB anaglyph, the proposed method also works in the CIELAB color space. Their differences include:

1. LAB anaglyph targets minimizing the L*a*b differences, while our method tries to match the perceptual color appearance attributes.
2. LAB anaglyph method formulates the problem as an optimization process. Our method can manipulate the lightness, saturation, and hue in a more controllable manner. For example, since the lightness significantly influences the retinal rivalry, we intentionally match the lightness of the left and right views to alleviate the retinal rivalry effect.
3. LAB anaglyph method needs iterative optimization. On the other hand, our method has a closed form solution, hence, is less computationally intensive.

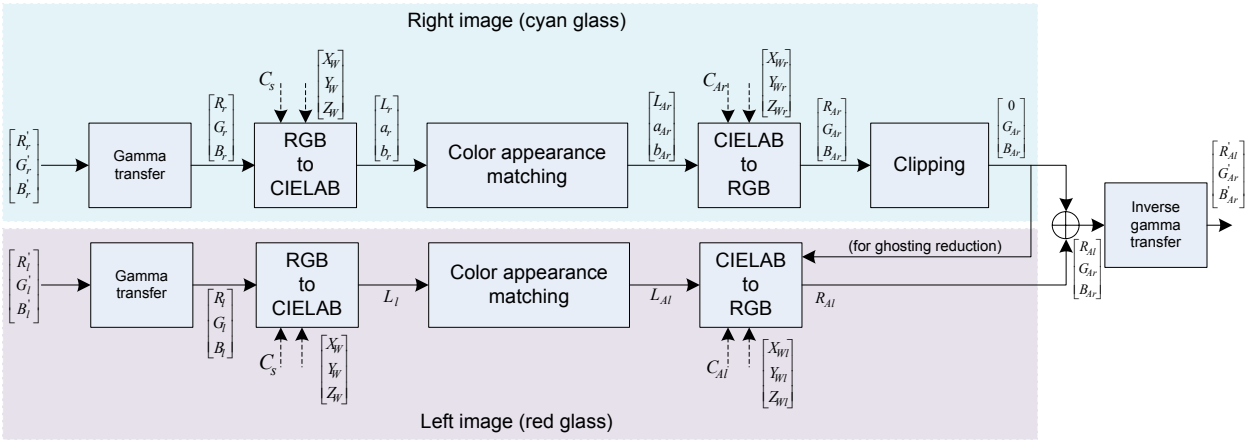

Figure 2: Systematic framework of the proposed algorithm.

In addition, the proposed method explicitly takes ghosting reduction into account. As to be elaborated in Section 3, we employ a subtractive ghosting reduction method. It is time-efficient and according to experimental results, it does reduce the ghosting artifacts to certain extent.

3. The Proposed Method

The systematic framework of the proposed algorithm is shown in Figure 2. In general, we convert the stereo pair from the device RGB color space to the CIELAB color space, and then calculate three perceptual color appearance attributes for each pixel position, including its lightness, saturation, and hue. We try to match these color appearance attributes to those of the perceived anaglyph, and finally convert them back into RGB. Detailed information on each processing module will be given below.

3.1. Gamma transfer

When visual signals are captured, gamma correction, i.e., a non-linear transformation of the captured RGB values, is typically performed in order to compensate the non-linearity[3] of the traditional CRT displays to achieve the correct color reproduction. Although modern displays show less or even no

[3]The non-linearity refers to the relationship between the device RGB values and the physical luminance of the display.

non-linearity, the same gamma correction for CRTs is still performed during the signal capture, because the other major and even more important purpose of the gamma correction is to minimize the perceptual distortions [21] introduced by signal compression or during signal communication. Therefore, the modern displays, such as LCDs, PDPs, DLPs, must simulate the gamma transfer function of CRT displays for the correct color reproduction. Therefore, in the proposed method we implement a gamma transfer function for CRTs. The 8-bit device RGB values $\{R', G', B'\}$ of the stereo pair are normalized by multiplying 1/255, and then transformed to $\{R, G, B\}$, as shown in Figure 2, using the sRGB gamma transfer function. The inverse gamma transfer (i.e., gamma correction) is performed after the derivation of RGB values of anaglyph images, and ultimately the gamma-corrected values will be scaled by multiplying 255. For the formulation of the forward and inverse sRGB gamma transfer functions, please refer to [21, 22].

3.2. Converting RGB to CIELAB

After simulating the gamma transfer, RGB values of the stereo pair are converted into L*a*b* values of the CIELAB color space. The conversion can be separated into two steps. The first step is to project the RGB values $\{R_l, G_l, B_l, R_r, G_r, B_r\}$ of the stereo pair[4] into the CIE XYZ color space:

$$C_s = \begin{bmatrix} 0.4243 & 0.3105 & 0.1657 \\ 0.2492 & 0.6419 & 0.1089 \\ 0.0265 & 0.1225 & 0.8614 \end{bmatrix} \tag{2}$$

$$\begin{bmatrix} X_r \\ Y_r \\ Z_r \end{bmatrix} = C_s \times \begin{bmatrix} R_r \\ G_r \\ B_r \end{bmatrix}, \begin{bmatrix} X_l \\ Y_l \\ Z_l \end{bmatrix} = C_s \times \begin{bmatrix} R_l \\ G_l \\ B_l \end{bmatrix} \tag{3}$$

The conversion matrix C_s is for typical LCD displays. In the second step, $\{X_l, Y_l, Z_l, X_r, Y_r, Z_r\}$ are converted into L*a*b* values, i.e., $\{L_l, a_l, b_l, L_r, a_r, b_r\}$, using equations below:

$$\begin{aligned} L_i &= 116 \cdot f(\tfrac{Y_i}{Y_W}) - 16 \\ a_i &= 500 \cdot [f(\tfrac{X_i}{X_W}) - f(\tfrac{Y_i}{Y_W})] \\ b_i &= 200 \cdot [f(\tfrac{Y_i}{Y_W}) - f(\tfrac{Z_i}{Z_W})] \end{aligned} \tag{4}$$

[4]Subscripts 'l' and 'r' indicate variables related to the respective left and right images of the stereo pair.

$$f(t) = \begin{cases} t^{1/3} & if\, t > 0.008856 \\ 7.787 \times t + 0.1379 & otherwise \end{cases} \quad (5)$$

where $i \in \{l, r\}$, and $\{X_W, Y_W, Z_W\}$ are XYZ values of the white point, i.e., $[X_W, Y_W, Z_W]^T = C_s \times [1, 1, 1]^T$.

3.3. Matching color appearance attributes in CIELAB color space

Given L*a*b* values of the stereo pair, our objective is to get $\{L_{Al}, a_{Al}, b_{Al}, L_{Ar}, a_{Ar}, b_{Ar}\}$ of the perceived anaglyph[5] which generate similar lightness, saturation and hue as those calculated from $\{L_l, a_l, b_l, L_r, a_r, b_r\}$. In our method, one (red) channel is used to present the left image and the other two channels (green and blue) are used to present the right one. Therefore, L*a*b* values of the perceived anaglyph must be intentionally chosen, so that, when converted back into RGB, the three-dimensional vector $\{L_{Al}, a_{Al}, b_{Al}\}$ can be represented by a single red value $\{R_{Al}\}$, and $\{L_{Ar}, a_{Ar}, b_{Ar}\}$ can be represented by $\{G_{Ar}, B_{Ar}\}$.

3.3.1. Right image processing

Firstly, we calculate the lightness, hue, and saturation of the right image of the stereo pair. According to the definition of the CIELAB color space, L* value, i.e., L_r, can be used to represent the lightness. Hue (H_r) and saturation (S_r) of the right image are represented by:

$$H_r = \frac{180}{\pi} \cdot [tan^{-1}(\frac{b_r}{a_r}) + \pi \cdot u(-a_r)] \quad (6)$$

$$S_r = \sqrt{a_r^2 + b_r^2} \quad (7)$$

where $u(\cdot)$ is the unit step function. $\{L_{Ar}, a_{Ar}, b_{Ar}\}$ represents the right view of the perceived anaglyph image in the CIELAB color space. A good choice of $\{L_{Ar}, a_{Ar}, b_{Ar}\}$ should satisfy two conditions: (1) they generate lightness, hue, and saturation values as close to L_r, H_r and S_r as possible; (2) in the RGB color space, they can be represented by $\{R_{Ar}, G_{Ar}, B_{Ar}\}$ with $R_{Ar} = 0$. For illustration, all $\{L_{Ar}, a_{Ar}, b_{Ar}\}$ that conform to the second condition are plotted in Figure 3(a). They are obtained by converting the 256×256 RGB values $\{R_{Ar} = 0, G_{Ar} = 0, 1, ..., 255, B_{Ar} = 0, 1, ..., 255\}$ into the CIELAB

[5]Subscripts '*Al*' and '*Ar*' indicate variables related to the left and right views of the anaglyph image, respectively.

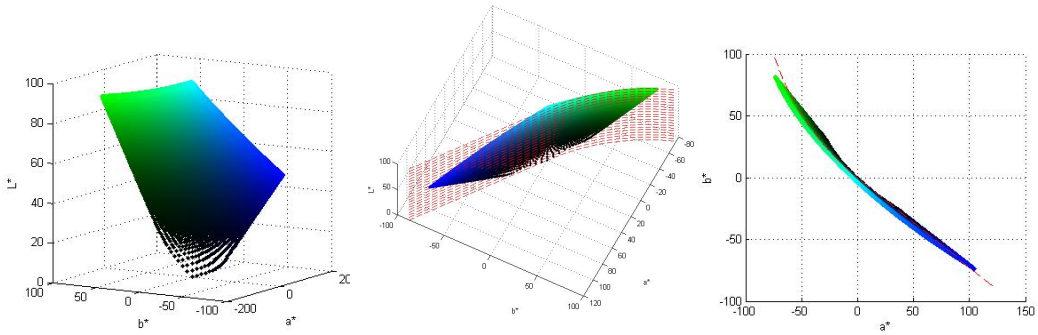

Figure 3: (a) 256×256 colors $\{R_{Ar} = 0, G_{Ar} = 0, 1, ..., 255, B_{Ar} = 0, 1, ..., 255\}$ in the CIELAB color space. (b) The approximation surface modeled by Eq. (9) and indicated by the red dashed lines. (c) Top views of the original and the approximation surface.

color space. The conversion follows the two steps described in Section 3.2. In this case, the conversion (RGB to CIE XYZ) matrix C_{A_r} is:

$$C_{A_r} = \begin{bmatrix} 0.0153 & 0.1092 & 0.1171 \\ 0.0176 & 0.3088 & 0.0777 \\ 0.0201 & 0.1016 & 0.6546 \end{bmatrix} \tag{8}$$

which is determined by spectral distributions of display primaries and also the transmission function of the right (cyan) lens. $[X_{Wr}, Y_{Wr}, Z_{Wr}]^T = C_{A_r} \times [1, 1, 1]^T$ is taken as XYZ values of the white point.

To satisfy the second condition, we need to ensure that $\{L_{Ar}, a_{Ar}, b_{Ar}\}$ lie in the surface shown in Figure 3(a). However, it will be very complex to precisely meet this requirement. Therefore, we approximate the original surface shown in Figure 3(a) by a simple surface empirically modeled as:

$$\begin{cases} b_{Ar} = k \cdot a_{Ar} & \textit{if } a_r > 0 \\ (a_{Ar} - a_c)^2 - (b_{Ar} - b_c)^2 = a_c^2 + b_c^2 & \textit{otherwise} \end{cases} \tag{9}$$

and $L_{Ar} \in [0, 100]$. The parameters are set as $k = -0.7273$, $a_c = 125$, $b_c = 172$. The dashed lines in Figure 3(b) represent the approximation surface. An animation version of Figure 3(b) can be found in the project website [23], from which it can be observed that the original surface shown in Figure 3(a) is nearly perpendicular to a*-b* plane. Figure 3(c) shows the

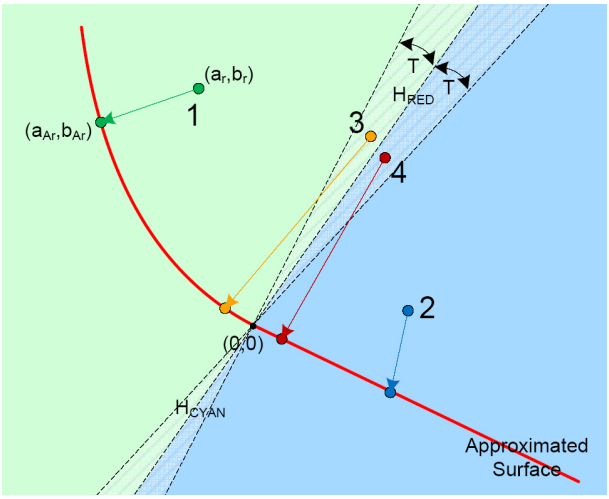

Figure 4: The red line resembles the top view of the approximation surface as shown in Figure 3(c). Examples 1-4 illustrate how Eqs. (10) and (11) project $\{a_r, b_r\}$ to $\{a_{Ar}, b_{Ar}\}$ in the CIELAB color space. Constant T is from Eq. (11).

top view. All $\{L_{Ar}, a_{Ar}, b_{Ar}\}$ derived below will lie in this approximation surface. When they are converted back into RGB, the resultant small red values (R_{Ar}) introduced by the approximation will be clipped to zero.

a_{Ar} and b_{Ar} specify the hue and saturation. Their values are determined by Eqs. (10) and (11):

$$\begin{cases} (a_{Ar} - a_c)^2 - (b_{Ar} - b_c)^2 = a_c^2 + b_c^2 \ \& \ a_{Ar} \leq 0 & \textit{if } H_r \geq H_{RED} \textit{ and } H_r \leq H_{CYAN} \\ b_{Ar} = k \cdot a_{Ar} \ \& \ a_{Ar} > 0 & \textit{otherwise} \end{cases} \tag{10}$$

$$\sqrt{a_{Ar}^2 + b_{Ar}^2} = \begin{cases} S_r \cdot |\frac{H_r - H_{RED}}{T}| & \textit{if } |H_r - H_{RED}| \leq T \\ S_r \cdot |\frac{H_r - H_{CYAN}}{T}| & \textit{if } |H_r - H_{CYAN}| \leq T \\ S_r & \textit{otherwise} \end{cases} \tag{11}$$

where $H_{RED} = 41.6°$, $H_{CYAN} = 221.6°$, $T = 15$. Figure 4 illustrates how the projection from $\{a_r, b_r\}$ to $\{a_{Ar}, b_{Ar}\}$ is performed according to Eqs. (10) and (11):

- Colors in the light green area are projected to the left part of the approximated surface (examples 1 and 3).
- Colors in the light blue area are projected to the right part of the approximated surface (examples 2 and 4).

- For colors in the flat area (without slashes), projections will generate the same saturation value as those of the right image of the stereo pair, i.e., $\sqrt{a_{Ar}^2 + b_{Ar}^2} = S_r$ (examples 1 and 2).
- For colors in the textured area (with slashes), $\sqrt{a_{Ar}^2 + b_{Ar}^2}$ will be smaller than S_r (examples 3 and 4).

In examples 3 and 4, the two colors appear similar in the right image of the stereo pair. If keeping their saturations during the projection, the resultant colors will be widely apart, introducing visual artifacts to the anaglyph image. By de-saturation as in Eq. (11), the projected colors will be located more closely.

L_{Ar} represents the lightness, and its value is determined by Eqs. (12) and (13):

$$L_{Ar} = \begin{cases} L_r \cdot (1 - P_{S_r} \cdot \frac{T - |H_r - H_{RED}|}{T}) & if\ |H_r - H_{RED}| < T \\ L_r & otherwise \end{cases} \tag{12}$$

$$P_{S_r} = \begin{cases} P_{max} & if\ S_r > S_{high} \\ P_{max} \cdot \frac{S_r - S_{low}}{S_{high} - S_{low}} & if\ S_r \leq S_{high}\ and\ S_r \geq S_{low} \\ 0 & if\ S_r < S_{low} \end{cases} \tag{13}$$

where $P_{max} = 0.4$, $S_{low} = 40$, $S_{high} = 50$, H_{RED} and T are the same as in Eqs. (10) and (11). It can be observed from Eq. (12) that for most colors the lightness remains unchanged after the projection, i.e., $L_{Ar} = L_r$. Special treatment is given to red-like colors, i.e., a maximum of 40% lightness reduction ($L_{Ar} = 0.6L_r$). This empirical operation intends to improve the chrominance accuracy of red-like colors (at the expense of increasing retinal rivalry and less lightness accuracy), which can help to improve the overall visual quality according to our viewing experiences. An example is given in Figure 5 which illustrates the improvement on chrominance accuracy. As shown in (12) and (13), the amount of lightness reduction is dependent on the hue and saturation values, i.e., H_r and S_r. The maximum reduction is reached when H_r equals H_{RED} and the saturation value is high ($Sr > S_{high}$). As given by Eq. (13), for low saturated colors ($S_r < S_{low}$), lightness reduction is not performed (i.e., $P_{S_r} = 0$). The purpose of this is to avoid abrupt lightness changes for low saturated colors. For the same reason, P_{S_r}slowly evolves from 0 to P_{max} when the saturation value S_r lies between S_{low} and S_{high}.

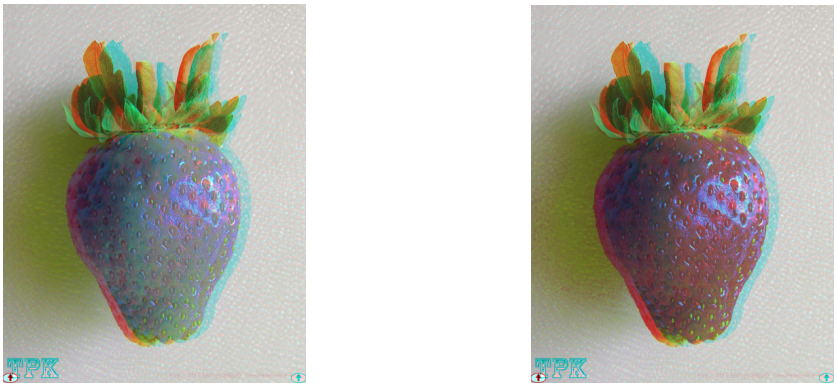

(a) (b)

Figure 5: A red strawberry: (a) before the lightness reduction of the right view, (b) after the lightness reduction.

3.3.2. Left image processing

To minimize retinal rivalry, left and right eyes should perceive identical lightness. Assuming that the stereo image pair is taken under well controlled conditions (e.g., same shutter speed, aperture, etc.), matching points in left and right views will have the same color. Therefore, to match the perceived lightness we simply make:

$$L_{Al} = L_l \tag{14}$$

where L_l represents the lightness of the left image of the stereo pair. In the final anaglyph, only the red channel is used to present the left view. We use it to reproduce the lightness L_{Al}. Hence, there is no need to calculate a_{Al} and b_{Al} anymore.

It should be noted that because lightness reduction is applied to red-like colors in the right image, as given by Eqs. (12) and (13), lightness matching for these colors cannot be achieved. Although this lightness reduction will cause more retinal rivalry and less lightness accuracy, it helps to improve chrominance accuracy of red-like colors, which we find empirically is useful for enhancing the overall visual quality of perceived images.

3.4. Converting CIELAB to RGB

For the right image, firstly $\{L_{Ar}, a_{Ar}, b_{Ar}\}$ are converted to $\{X_{Ar}, Y_{Ar}, Z_{Ar}\}$ using Eqs. (15) and (16):

$$\begin{array}{rcl} X_{Ar} & = & X_{Wr} \cdot f^{-1}(\frac{L_{Ar}+16}{116} + \frac{a_{Ar}}{500}) \\ Y_{Ar} & = & Y_{Wr} \cdot f^{-1}(\frac{L_{Ar}+16}{116}) \\ Z_{Ar} & = & Z_{Wr} \cdot f^{-1}(\frac{L_{Ar}+16}{116} - \frac{b_{Ar}}{200}) \end{array} \tag{15}$$

$$f(t)^{-1} = \begin{cases} t^3 & if\, t > 0.2069 \\ 0.1284 \times (t - 0.1379) & otherwise \end{cases} \tag{16}$$

Then $\{X_{Ar}, Y_{Ar}, Z_{Ar}\}$ are converted to RGB values by:

$$\begin{bmatrix} R_{Ar} \\ G_{Ar} \\ B_{Ar} \end{bmatrix} = C_{Ar}^{-1} \times \begin{bmatrix} X_{Ar} \\ Y_{Ar} \\ Z_{Ar} \end{bmatrix} \tag{17}$$

As discussed in Section 3.3, the small R_{Ar} will be clipped to zero, leaving the right view represented by $\{G_{Ar}, B_{Ar}\}$ only.

For the left image, firstly L_{Al} is converted to Y_{Al}:

$$Y_{Al} = Y_{Wl} \cdot f^{-1}(\frac{L_{Al}+16}{116}) \tag{18}$$

where Y_{Wl} is one of XYZ values of the white point, i.e., $[X_{Wl}, Y_{Wl}, Z_{Wl}] = C_{Al} \times [1,1,1]^T$, and the conversion matrix for the left lens is:

$$C_{Al} = \begin{bmatrix} 0.1840 & 0.0179 & 0.0048 \\ 0.0876 & 0.0118 & 0.0018 \\ 0.0005 & 0.0012 & 0.0159 \end{bmatrix} \tag{19}$$

Given Y_{Al}, R_{Al} can be calculated by:

$$R_{Al} = \frac{max(Y_{Al} - 0.0118G_{Ar} - 0.0018B_{Ar}, 0)}{0.0876} \tag{20}$$

where $0.0118G_{Ar}$ and $0.0018B_{Ar}$ quantify the luminance leakage for the left eye, which are subtracted from the intended luminance Y_{Al}. This is a subtractive ghosting reduction method. If the matrix C_{Al} is accurate, it can guarantee a perfect ghosting inhibition in regions where Y_{Al} is larger than

the luminance leakage. As discussed in [19, 20], for complete ghosting elimination it is required to suppress the image dynamic range, which will degrade visual quality intuitively.

It can be observed from Eq. (8) that compared to that of the left eye, the luminance leakage of the right eye will be far less severe. In [20], it is also claimed that for red-cyan glasses the right eye suffers less from the luminance leakage (about 1/7 of that of the left eye). Therefore, in the proposed algorithm ghosting reduction is implemented for the left image only.

Eventually, right and left RGB values are combined together as $\{R_{Al}, G_{Ar}, B_{Ar}\}$. Each element is clipped into the range 0 to 1. They are gamma corrected, and finally scaled by multiplying 255.

3.5. Parameterization

For color space conversion and ghosting reduction, values of the matrices C_s, C_{Al}, and C_{Ar} are cited from [1]. These parameters are fixed and should be suitable for typical LCD displays and red-cyan glasses. If they are refined by true properties of the display and glasses, or by simple subjective tests as in [20], the performance will be further optimized. The other parameters are set manually. Values of k, a_c, b_c are chosen so that top views of the original and approximated surfaces as introduced in Section 3.3 overlap closely. S_{low}, S_{high}, P_{max}, and T are determined empirically, based on a few stereo pairs which are excluded from the following subjective performance evaluation.

4. Performance Evaluation

We conduct subjective tests to evaluate performances of four anaglyph algorithms, i.e., Color anaglyph, XYZ anaglyph [5], LAB anaglyph [1], and the proposed anaglyph. To the best of our knowledge, this is the first subjective test described in the literature to evaluate the visual quality of anaglyph images. Experimental data can be downloaded from the project website [23].

4.1. Overall performance

We download 25 stereo image pairs from the Internet [24, 25], which cover a wide range of colors and scene types. They are down-scaled to standard-definition (around 800×600) while keeping their aspect ratios. Right images of these stereo pairs are shown in Figure 6. For each stereo pair, four anaglyph images, i.e., Color anaglyph, XYZ anaglyph, LAB anaglyph, and

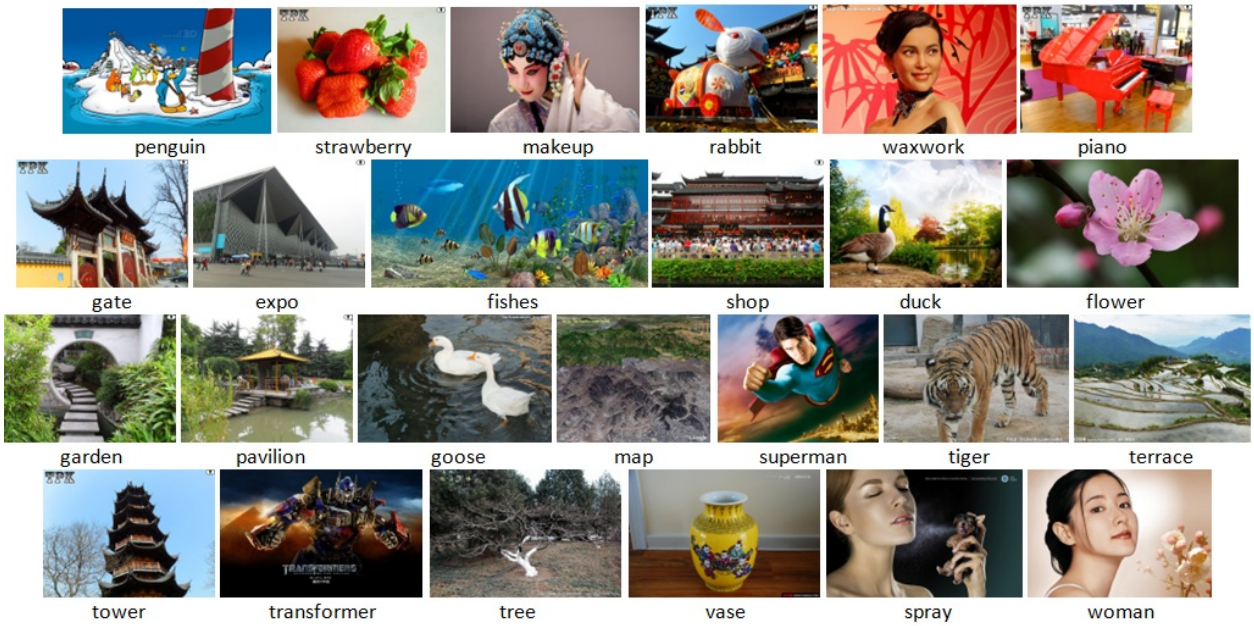

Figure 6: Right images of the 25 stereo pairs used in the subjective tests.

the proposed one, are presented simultaneously as illustrated by Figure 7. This side-by-side arrangement is to speed up the comparison process in order to lessen the fatigue of subjects. We implemented Color and XYZ anaglyph generation algorithms. Implementation of the XYZ anaglyph generation algorithm strictly follows instructions from [22]. The code of LAB anaglyph was provided by its author.

Evaluation is performed in a room with fluorescent lights. The display monitor is a 24" 1920×1200 Dell LCD display (2407WFPB), and the viewing distance is about 3 times the screen height. The red-cyan glasses are the NVIDIA 3D Vision Discover. Totally 20 subjects (non-experts) attended the tests. They have normal vision (with or without corrective glasses) and have passed the color blindness test. For each stereo pair, each subject is asked to assess the visual quality of four anaglyph images which are displayed simultaneously. The assessment is reported on a five-point scale: 5-Excellent, 4-Good, 3-Fair, 2-Poor, and 1-Bad. To lessen fatigue, subjects tell their opinions to another person who is responsible for recording the scores. There is no limitation on the viewing duration, and subjects are encouraged to express their feelings about what factors they attribute the quality to. The order of

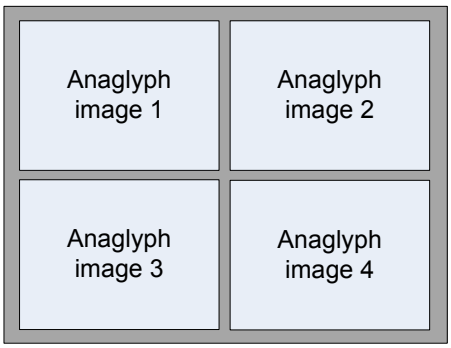

Figure 7: Four anaglyph images are displayed simultaneously in the original resolution.

the 25 images and positions of the four anaglyph methods are randomized for each subject. Each test lasts around 30 minutes. At the beginning, three anaglyph images are arranged as a training process to familiarize the subjects with the anaglyph 3D viewing and test the possible stereo blindness of the subjects.

We use the proposed method as a reference. Subjective ratings of the proposed method are subtracted from those of the corresponding Color, XYZ, and LAB anaglyphs. Difference values are processed using the method described in the BT. 500 standard [26] to derive the difference mean opinion scores (DMOS) and 95% confidence interval for each anaglyph image. The β_2 test suggested in [26] is used to identify the subjects whose quality judgments deviate from the distribution of the normal scores significantly. Two subjects are rejected.

Figure 8 shows final results of 75 anaglyph images. Red, green, and blue circles indicate DMOS of Color, XYZ, and LAB anaglyphs, respectively. The vertical line passing through each circle represents the 95% confidence interval. Larger mean score denotes better visual quality. With the circle below the dashed zero line, it means that the proposed method demonstrates better visual quality. In general, it can be observed from Figure 8 that the proposed method achieves very good performance. Most circles are below the dashed zero line.

Table 1 gives a brief summary of the performance comparison. For each method, the 1^{st} row shows the DMOS on the 25 images (higher value indicates better performance), and the $2^{nd}/3^{rd}/4^{th}$ row lists the number of rank in top 1/2/3 (i.e., a count for how many times the method is ranked first/second/third). Notice that there are ties for the best performer, so the

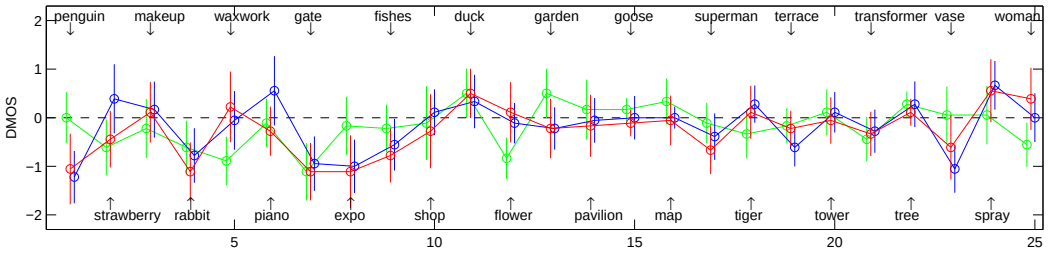

Figure 8: Performance comparison on 25 images among four anaglyph methods using the proposed one as a reference. The dashed zero line: proposed method; red: Color anaglyph; green: XYZ anaglyph; blue: LAB anaglyph. Each circle corresponds to an anaglyph image. The vertical line passing through each circle represents the 95% confidence interval. Larger mean score indicates better visual quality. The proposed method produces better quality if the circle is below the dashed zero line.

Table 1: A brief summary of the performance comparison among four anaglyph generation methods, i.e., Color, XYZ, LAB, and the proposed method, on 25 images.

	Color	XYZ	LAB	Proposed
Mean score on 25 images	-0.260	-0.176	-0.173	0
No. of rank in top 1	4	9	8	8
No. of rank in top 2	7	14	13	19
No. of rank in top 3	15	18	22	22

sum of values in the 2^{nd} row does not add up to 25. Similarly, for the 3^{rd} or 4^{th} row, the sum of values does not add up to 50 or 75 either. In general, it can be seen from Table 1 that the proposed method performs relatively well on this data set.

However, it is also evident that performances are content-dependent. No method consistently outperforms another on all images, and the 95% confidence intervals in many cases are large, as shown in Figure 8. According to comments from subjects collected during tests, there is a variation between individuals about which factor is considered more important for good visual quality, e.g., less retinal rivalry, or better chrominance accuracy, etc. The large 95% confidence intervals shown in Figure 8 can be attributed to this variation.

4.2. Chrominance accuracy, retinal rivalry and ghosting effect

Five images are selected in another experiment to evaluate the image quality regarding specific visual factors, e.g., chrominance accuracy[6], retinal rivalry, and ghosting effect. To analyze the reason why one method has particularly good performance on a certain image, we select images based on subjective quality evaluation results shown in Figure 8. Four images, i.e., *women*, *garden*, *strawberry* and *gate*, are chosen, because they are associated with best performances of the four anaglyph methods, i.e., Color, XYZ, LAB, and the proposed one, respectively. One additional image, i.e., *penguin*, is selected because it is commonly used for comparing anaglyph methods [25].

The main differences between this experiment and the previous one described in Section 4.1 include:

(1) Subjects need to give four quality scores for each anaglyph image, evaluating its chrominance accuracy, retinal rivalry, ghosting, and overall quality. Therefore, in the training stage, to each subject we explain the concepts of these visual phenomena by using image examples. These image examples do not include the five images used in the testing stage.

(2) The original image is shown to each subject, so that the subject can memorize its color and evaluate the chrominance accuracy of the anaglyph images. Specifically, for each of the five images in the test, the left view of the stereo image pair is shown in 2D to the subject. He/She can take as much time as he/she needs to memorize the colors. Then, he/she is asked to put on the 3D glasses and evaluate four anaglyph images which are arranged in the way shown in Figure 7. To prevent memory fading, the chrominance accuracy is evaluated first, followed by retinal rivalry, ghosting, and overall quality.

The other experimental procedures are similar with those described in Section 4.1. For each subject, the whole session needs around 20 to 30 minutes to complete. 18 subjects in total participate in the experiment. The assessment is also reported on a five-point scale. As in Section 4.1, subjective ratings of our anaglyph images are subtracted from those of the other anaglyph methods. The difference values are processed using the method

[6]Color accuracy include both lightness and chrominance accuracy. In this experiment, only chrominance accuracy is tested, since we found in the previous experiment that our method may not be good at chrominance reproduction.

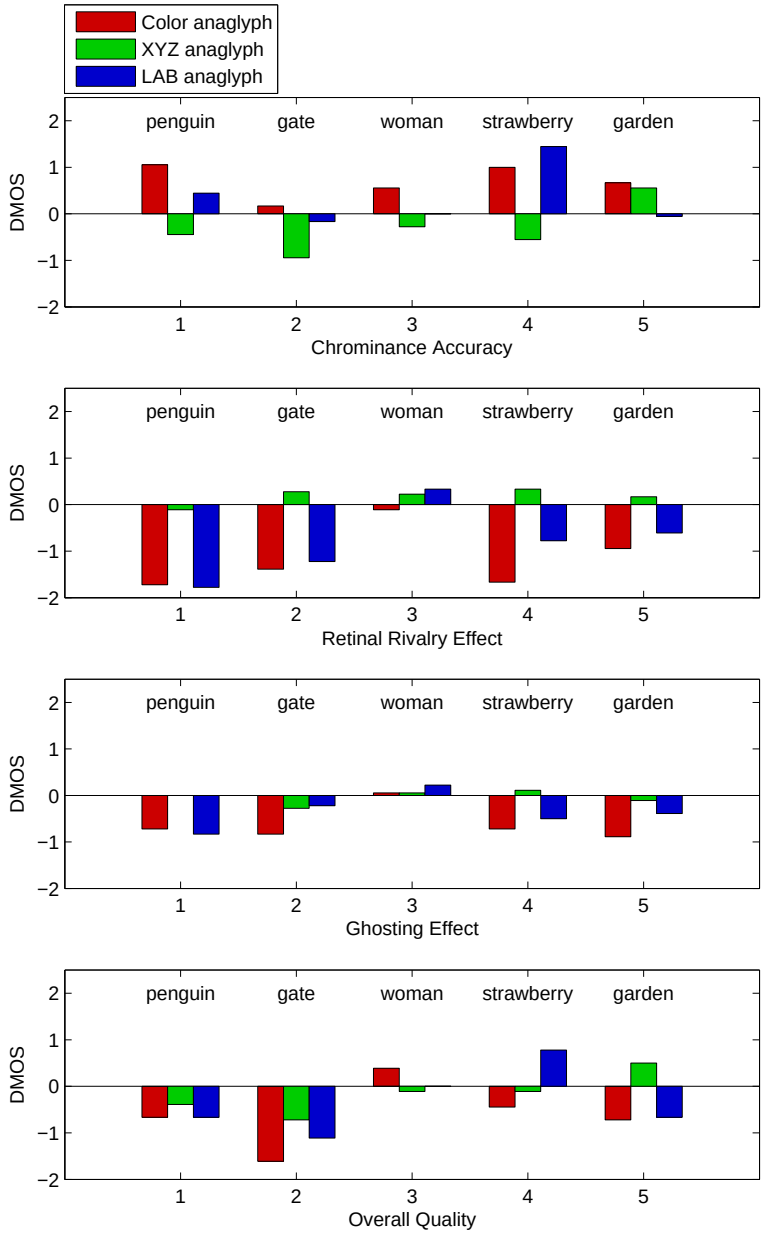

Figure 9: From top to bottom, subfigures demonstrate evaluation results for chrominance accuracy, retinal rivalry, ghosting effect, and overall visual quality. The horizontal axis indicates different images, while the vertical axis indicates DMOS. Higher DMOS, better chrominance accuracy/less retinal rivalry/less ghosting effect/better overall quality. The red, green and blue bars are associated with Color, XYZ, and LAB anaglyph methods, respectively.

described in the BT. 500 standard [26] to derive the difference mean opinion score (DMOS). The β_2 test [26] is used to identify outlier subjects. In this experiment, no subject is rejected.

Figure 9 shows experimental results. From top to bottom, subfigures demonstrate evaluation results for chrominance accuracy, retinal rivalry, ghosting effect, and overall visual quality. The horizontal axis indicates different images, and vertical axis indicates DMOS − higher DMOS, better chrominance accuracy (less retinal rivalry, less ghosting effect, or better overall quality). Red, green and blue bars are respectively associated with Color, XYZ, and LAB anaglyph methods. Positive DMOS means the corresponding method performs better than the proposed one, while negative DMOS means that it is outperformed by the proposed one.

It can be observed from Figure 9 that regarding chrominance accuracy, Color anaglyph outperforms the proposed method on all five images. It is the best performer for *penguin*, *gate*, *women*, and *garden*, and second best for *strawberry*. LAB anaglyph is also relatively good at chrominance reproduction, shown by *penguin* (a very colorful image) and especially *strawberry*. The XYZ anaglyph performs relatively worse than others in terms of the chrominance accuracy, but better at presenting greenish colors, as shown in the test image *garden*.

Regarding the retinal rivalry effect, we can see that in general XYZ and our method outperform Color and LAB anaglyph methods obviously except for the test image *women* in which all methods generate little retinal rivalry. When comparing Color with LAB anaglyph, it can be seen that in many cases (4 out of 5) LAB anaglyph is better at reducing retinal rivalry.

Regarding the ghosting effect, there is less variation between different methods compared to that of chrominance accuracy and retinal rivalry. Generally, the proposed method seems to perform the best, closely followed by XYZ, LAB and lastly Color anaglyph.

Comparing Figure 8 and 9, we can see that overall quality scores in these two figures exhibit similar trends. In particular, the top performing method remains the same for each of the five tested images. On the other hand, differences between these two sets of results are due to the variation of opinions between different subjects as analyzed in Section 4.1, and also from the fact that this experiment uses the original image as a reference, while the previous one does not. The use of reference images does have influence the overall quality judgement. As exemplified in a very colourful image *penguin*, since subjects can refer to the original colors, the large overall quality dif-

ferences shown in Figure 8 now diminish in Figure 9. The advantages of less retinal rivalry of XYZ and the proposed method are weakened by their disadvantages in chrominance reproduction. However, retinal rivalry indeed plays a very important role in the overall quality, despite the presence of reference colors. We simply calculate the linear correlation coefficient (LCC) between different groups of quality scores. The LCC between overall quality scores and chrominance accuracy scores is 0.319, while the LCC between overall quality scores and retinal rivalry scores is 0.511, which means that retinal rivalry may be more closely related to the overall quality of perceived anaglyph images. However, this does not mean chrominance accuracy is not important. It can be observed from Figure 9 that when retinal rivalry is subtle, chrominance will dominate the overall quality judgment, as exemplified by *women* and *strawberry*.

It should be noted that limited by the experiment duration, the above analysis is only based on five images which may be inadequate. Future works need to be done for a more detailed statistical analysis.

4.3. Complexity

Among the four anaglyph generation algorithms, Color anaglyph is the simplest one. If disregarding the gamma transfer, XYZ anaglyph is as time-efficient as Color anaglyph. LAB anaglyph has the greatest complexity, since it involves a non-linear transform in the minimization process, as discussed in Section 2, which needs to be solved iteratively. Compared to LAB anaglyph, the proposed method is much simpler. Without specific optimization, the Matlab code of the proposed method needs about two seconds to process an 800×600 sized image.

5. Conclusion

In this paper, a new algorithm is proposed for anaglyph image generation. Distinguished from the existing techniques which aim at matching the perceived anaglyph image to the stereo pair in terms of RGB, XYZ or L*a*b* values, the proposed method tries to match the three perceptual color appearance attributes, i.e., lightness, hue, and saturation, since they can more precisely define the HVS color perception. Subjective tests are conducted to evaluate performances of the various anaglyph generation methods. It turns out that the proposed algorithm performs quite well. The subjective test also reveals that the performance is content-dependent. Besides, it shows that

there is a large variation between individuals about which factor is considered more important in the evaluation of visual quality of anaglyph images. A further point to note is that incorporating color enhancement into the proposed anaglyph generation method is extremely easy by tuning the lightness and saturation values.

References

[1] D.F. McAllister, Y. Zhou, and S. Sullivan, "Methods for computing color anaglyphs", Stereoscopic Displays and Applications XXI, vol. 7524, 2010.

[2] L.M.J. Meesters, W.A., Ijsselsteijn, and P.J.H. Seuntiens, "A survey of perceptual evaluations and requirements of three-dimensional TV", IEEE Transactions on Circuits and Systems for Video Technology, vol. 14, no. 3, pp. 381-391, 2004.

[3] R.Z. Zeng, and H.Z. Zeng, "Printing anaglyph maps optimized for display", Proceedings of the SPIE, vol. 7866, pp. 78661S-78661S-5, 2011.

[4] M.J. Tovee, "Brain and space", An Introduction to the Visual System (2nd Edition), Cambridge University Press, 2008.

[5] E. Dubois, "A projection method to generate anaglyph stereo images", IEEE International Conference on Acoustics, Speech, and Signal Processing, vol. 3, pp. 1661-1664, 2001.

[6] A.J. Woods, and T. Rourke, "Ghosting in anaglyphic stereoscopic images", Stereoscopic Displays and Virtual Reality Systems XI, vol. 5291, pp. 354-365, 2004.

[7] A.J. Woods, "Understanding Crosstalk in Stereoscopic Displays", (Keynote Presentation) at 3DSA (Three-Dimensional Systems and Applications) conference, Tokyo, Japan, 2010.

[8] J. Konrad, B. Lacotte, and E. Dubois, "Cancellation of image crosstalk in time-sequential displays of stereoscopic video", IEEE Transactions on Image Processing, vol. 9, no. 5, pp. 897-908, 2000.

[9] Trioscopic 3D, `http://www.trioscopics.com/`

[10] ColorCode 3D, `http://www.colorcode3d.com/`

[11] Robin Lobel, Magenta-cyan anaglyphs, http://www.divideconcept.net/papers/MCA-RL09.pdf

[12] Infitec Dualcolor3D, http://www.infitec-global-sales.com/english/infitec-definiton.htm

[13] 3DTV, http://3dtv.at/Knowhow/AnaglyphComparison_en.aspx

[14] Z. Zhang, and D.F. McAllister, "A uniform metric for anaglyph calculation", Stereoscopic Displays and Virtual Reality Systems XIII, vol. 6055, pp. 5513-5513, 2006.

[15] M.D. Fairchild, "Color Appearance Models (2nd Edition)", Wiley-IS&T, Chichester, UK, 2005.

[16] I. Ideses, and L. Yaroslavsky, "Three methods that improve the visual quality of colour anaglyphs", Journal of Optics A: Pure and Applied Optics, vol. 7, pp. 755-762, 2005.

[17] W. Alkhadour, et al., "Creating a Color Anaglyph from a Pseudo-Stereo Pair of Images", 4th International Conference On Information Technology, Amman, Jordan, June 2009.

[18] A.J. Chang, et al., "Ghosting reduction method for color anaglyphs", Proceedings of the SPIE, vol. 6803, pp. 68031G-68031G-10, 2008.

[19] V. Tran, "New Methods for Rendering Anaglyphic Stereoscopic Images on CRT Displays and Photo-Quality Inkjet Printers", M.S. Thesis, University of Ottawa, 2005.

[20] H. Sanftmann, and D. Weiskopf, "Anaglyph Stereo Without Ghosting", Computer Graphics Forum, vol. 30, Issue 4, pp. 12511259, June 2011.

[21] C. Poynton, "Gamma", A Technical Introduction to Digital Video, Wiley, New York, 1996.

[22] E. Dubois, "Conversion of a Stereo Pair to Anaglyph with the Least-Squares Projection Method", http://www.site.uottawa.ca/~edubois/anaglyph/LeastSquaresHowToPhotoshop.pdf, 2009

[23] IVP anaglyph image database, http://www.ee.cuhk.edu.hk/~snli/anaglyph_database.htm

[24] 3D China, http://www.china3-d.com/3dclub/

[25] SWell3D, http://www.swell3d.com/color-anaglyph-methods-compare.html

[26] ITU-R Recommendation BT.500-11, "Methodology for the subjective assessment of the quality of television pictures", ITU, Geneva, Switzerland, 2002.